

15. INVESTIGATION OF CRETACEOUS AND TERTIARY KEROGENS IN SEDIMENTS OF THE WEDDELL SEA¹

K.F.M. Thompson² and W. G. Dow³

ABSTRACT

Seventy-one samples from nine sites were analyzed for total organic carbon (TOC). Fifty-six samples, containing 0.2% or more TOC, were evaluated by Rock-Eval to assess the nature of their kerogen and its petroleum source potential. Visual kerogen studies were carried out. Petroleum potential was encountered only in Valanginian calcareous claystones at Hole 692B close to the margin of Dronning Maud Land. A section of 44.7 m was penetrated. The unit possesses a revised mean TOC of 9.8% and petroleum potential of 43.2 kg/Mg, relatively high values in comparison to other Cretaceous anoxic oceanic sections and the totality of petroleum source rocks. At Sites 689 and 690, extremely low TOC levels, mean 0.07%, preclude kerogen analysis. Kerogens in Eocene to Pliocene sediments of the central and western Weddell Sea (Sites 694, 695, 696, and 697) are similar everywhere, largely comprising brown to black, granular, amorphous material of high rank, and generally possessing several reflectance populations of vitrinite particles. The latter are interpreted as indicative of the recycling of sediments of a variety of levels of thermal maturity.

ANALYTICAL PROCEDURES

The suite of samples examined in this study, largely 4-cm sections of whole core, comprises those obtained during Ocean Drilling Program (ODP) Leg 113 for purposes of later detailed analysis of extracted bitumens. Cores were sampled upon recovery, avoiding any possible lipid or hydrocarbon contamination, sealed in oven-fired glass jars, and immediately frozen. They were maintained in a frozen condition until analysis. After several months, however, analyses of headspace gases revealed the presence of low molecular weight contaminants which had evidently diffused out of the polymeric gasket sealant on the lids of the jars.

Analytical results reported here do not duplicate those made on the *JOIDES Resolution*, except in the case of Hole 692B which penetrated a Cretaceous (Valanginian) section of unusual interest. The results will be of value in conjunction with the bituminological studies to be published elsewhere. The present auxiliary studies comprise standard kerogen evaluations involving measurement of total organic carbon (TOC%), Rock-Eval pyrolytic parameters, microscopic visual determination of kerogen components, thermal history on the basis of color, and instrumentally determined reflectance values of disseminated vitrinite particles.

Total organic carbon (TOC) was measured with a LECO EC-12 carbon analyzer. Samples of 0.2 g were ground to pass a 60 mesh (250 μ m) sieve, treated with concentrated hydrochloric acid to remove carbonate minerals, and washed as well as filtered into a porous crucible.

Pyrolytic analyses were carried out with a Rock-Eval II (Delsi Inc.), operated in a mode (Cycle 1) which provides four fundamental parameters: S_1 (representing free and adsorbed hydrocarbons); S_2 (pyrolytic hydrocarbons); S_3 (pyrolytic organic carbon dioxide); and T_{max} (the temperature of maximum pyrolytic hydrocarbon yield). Hydrocarbons are detected by a flame ion-

ization detector, and carbon dioxide by a thermal conductivity detector.

The fundamental parameters are employed to obtain derived parameters. These are the Hydrogen Index (HI), or ($S_2 \times 100/\text{TOC}$) mg (hydrocarbons)/g (carbon); the Oxygen Index (OI), or ($S_3 \times 100/\text{TOC}$) mg (CO_2)/g (carbon); and the Performance Index (PI) or $S_1/(S_1 + S_2)$. HI assesses petroleum-generating potential, deemed significant if the value exceeds 300 mg/g, given an OI value less than approximately 50 mg/g. OI assesses the oxygen concentration of the kerogen, significant only in terrestrial, lignitic materials. PI is determined by thermal history, as is T_{max} . Both increase during catagenesis.

Optical microscopy employing a Zeiss Universal microscope at a magnification of 500-fold was carried out on isolated kerogens, both in reflected and transmitted white light and in ultraviolet light. A sample of ground sediment is treated successively with hydrochloric, hydrofluoric, and hot hydrochloric acids to release kerogen. The latter is concentrated by flotation in a zinc bromide solution of specific gravity 2.0, separating it from accompanying pyrite. For reflectance studies kerogen is mounted in epoxy resin and polished; for transmitted light examination it is mounted in Elvacite-2040 (a DuPont synthetic resin).

RESULTS

Sites 689 and 690

Table 1 presents total organic carbon determinations representing sediments from Holes 689B, 690C, and 693A. In all cases TOC fails to exceed 0.2%. At such low concentrations the performance of the Rock-Eval device is impaired (Deroo et al., 1983; and shipboard data, Barker, Kennett, et al., 1988).

Six samples were acidified for kerogen extraction. Again, none yielded sufficient material for meaningful analysis. No further information relevant to Sites 689 and 690 was obtained.

Hole 692B

Hole 692B was drilled on a shelf of the continental rise, the Explora Wedge, off Kapp Norvegia in the eastern Weddell Sea. The site is located in 2885.3 m of water on a shoulder of Wegener Canyon, close to the margin of Dronning Maud Land.

The cored interval totaling 97.9 m yielded 29.3 m of recovered sediment (29.9%). The section below 53.2 mbsf was assigned to Lithostratigraphic Unit III of Valanginian age on the basis of

¹ Barker, P. F., Kennett, J. P., et al., 1990. *Proc. ODP, Sci. Results*, 113: College Station, TX (Ocean Drilling Program).

² Texas A&M University, Department of Oceanography, Geochemical and Environmental Research Group, 10 S. Graham Road, College Station, TX 77840. Current address: BP Exploration Inc., Westport Lab, P.O. Box 4587, Houston, TX 77210.

³ D.G.S.I., Inc., Suite 402, 1544 Sawdust Road, The Woodlands, TX 77387.

Table 1. Determination of organic carbon, levels below 0.2%, Sites 689, 690, and 693.

Core, section, interval (cm)	Depth (mbsf)	TOC (wt%)
689B-5H-1, 46-150	35.26	0.09
689B-22X-4, 125-129	203.25	0.05
689B-25X-4, 125-129	232.35	0.12
689B-28X-3, 125-129	259.85	0.09
689D-12H-4, 146-150	130.06	0.04
690C-4H-1, 146-150	26.96	0.06
690C-6H-1, 146-150	46.36	0.05
690C-9H-1, 146-150	75.46	0.05
690C-11X-3, 125-129	208.45	0.08
690C-14X-4, 125-129	238.95	0.03
690C-17X-2, 120-124	264.50	0.07
690C-20X-4, 125-129	296.55	0.16
693A-6R-4, 128-132	46.88	0.13
693A-9R-4, 128-132	75.88	0.13
693A-4R-3, 125-129	26.15	0.10
693B-9X-3, 125-129	301.05	0.16
693B-12X-3, 125-128	330.05	0.15
693A-18R-3, 128-132	116.18	0.19
693A-28R-3, 128-132	257.88	0.10

palynomorphs (B. Mohr, this volume, chapter 29). A thickness of 44.7 m of Unit III was penetrated, of which 22.18 m was recovered (49.6%). Three lithologies were represented. According to the site report these are claystones (Core 113-692B-7R), underlain by nanofossil-bearing claystones and clayey chinks with laminae of tan volcanic ash (Cores 113-692B-8R to -10R), and carbonate-bearing, nanofossil-bearing clayey mudstones (Core 113-692B-12R). All of the mudstones are either massive or finely laminated and exhibit no bioturbation. They varied in color while wet from black (5Y 2.5/1), to very dark gray (10YR 3/1), dark olive gray (5Y 3/2), and olive gray (5Y 4/2). There are no specific color-lithology associations. Shell fragments, including *Inoceramus*, are abundant throughout. These indications are of an anaerobic to dysaerobic marine depositional site, distal to a terrestrial sediment source.

The carbonate contents of the claystones, measured by acidification and coulometric detection of carbon dioxide in the shipboard laboratory, ranged from 0.83% (Sample 113-692B-7R-1, 115-116 cm) to 41.87% (Sample 113-692B-9R-1, 32-33 cm) averaging $17.17\% \pm 12.97\%$.

Rock-Eval data representing Lithostratigraphic Unit III were obtained both in the geochemical laboratory of the *JOIDES Resolution* and that of the authors. Analyses of 10 samples were replicated, yielding results that are in poor agreement. It is suggested that the grand means of the replicates (Table 2) provide the optimum representation of the kerogen type and the petroleum potential of the section. Both Rock-Eval instruments are identical Delsi Series II instruments with TOC capability. However, TOC was determined independently in both instances.

Organic carbon was determined shipboard in two stages. Carbonate carbon was initially removed by hydrochloric acid treatment. Organic carbon remaining was determined by combustion in a Coulometrics, Inc. 5010-5020 Total Carbon Apparatus. As stated above, our carbon analyses employed a LECO EC-12. Expressing the difference between means as a percentage of the grand mean, Table 2 shows that the shipboard measurements exceed the LECO results by 10.1%.

A further discrepancy between the suites of data is represented in the Rock-Eval S_2 results (Table 2), expressed in milligrams of pyrolytic hydrocarbons per gram of rock. Shipboard data once more exceed those of the authors. The means differ by 51.3% of the grand mean. In calculations of Hydrogen Index (HI) values, the principal indicators of merit, the errors are

somewhat compensatory, so that the shipboard mean HI exceeds that of the authors by 39.8% of the grand mean.

Table 3 presents seven further Rock-Eval analyses of Hole 692B Unit III sediments. Two of these, Sample 113-692B-8R-1, 46-47 cm and Sample 113-692B-8R-2, 25-26 cm, represent laminae or lenses principally composed of volcanic ash. They average 1.32% TOC. The claystones in this subset average 7.52% TOC; average HI = 375 mg HC/g C.

Despite the unexplained discrepancies between the shipboard and present analyses, the grand mean data of Table 2 retain the indications of a thick (44.7 m) sequence of petroleum source rocks of excellent quality. Means of the duplicate values of HI, OI, and T_{max} are plotted in Figures 1 and 2.

Table 4 presents visual kerogen information relevant to all analyzed samples. The four samples representing Hole 692B contain dominant amorphous kerogen with 5%-25% exinite and traces to 10% vitrinite. Both exinite and vitrinite are indicative of a subordinate input of terrestrial organic matter. Amorphous kerogen is, in this instance, attributed to phytoplanktonic sources, confirmed by Rock-Eval data. The kerogen is brown to black, orange fluorescent in ultraviolet light, locally gray to brown. Fragments of algae and acritarchs fluoresce yellow and orange. Vitrinite reflectance measurements (R_o) are necessarily few. Individual sample means are therefore questionable, ranging from interpreted levels of 0.42%-0.62%. The overall mean of 10 reliable measurements (Fig. 3) is $0.52\% \pm 0.10\%$. Estimates of the level of thermal alteration, employing an index value (TAI) usually based upon spore coloration, were based in this instance upon kerogen color. At any given maturity, kerogens are somewhat darker than spores and pollens. Derived values are preceded by an asterisk to indicate this distinction in appropriate instances. The kerogen value in Hole 692B samples, *2, is in agreement with the interpreted vitrinite reflectance level. Visual examination confirms the instrumental information indicating a good quality source rock in an immature condition but approaching the level of rapid increase in bitumen generation ($\sim 0.6\% R_o$).

Site 693

Site 693 is located 30 km west-southwest of Site 692, 10 km southwest of the rim of Wegener Canyon, in 2359 m of water. Hole 693A was rotary drilled to 483.9 mbsf. Seven lithostratigraphic units were penetrated. As described in the site report, these comprise Units I, II, and upper IIIA, Pleistocene and Pliocene; lower IIIA, IIIB, and upper IIIC, Miocene; lower IIIC, IV, and V, Oligocene; VI and VII, Santonian, Aptian-Albian.

Organic geochemical interest centers on the Aptian-Albian Unit VII, top at 409.0 mbsf based on electric log measurements. Sediments are dominantly claystones with minor mudstones, very low in biogenic components, pyritic, with common shell fragments, dark in color, ranging from black and very dark gray, to dark gray. Organic carbon contents are high, commonly exceeding 2% (shipboard data), yet Rock-Eval measurements reveal that virtually no petroleum source potential remains, a condition attributed to syndepositional oxidation.

Table 4 presents visual kerogen data. A clear-cut bipartite division of the cored section is possible on the basis of kerogen type. A younger unit, comprising at least Lithological Units I through IIIC, middle to early Miocene through Pleistocene, represented by samples from and above Core 113-693A-28R, is strongly dominated by vitrinite. An older unit of Aptian-Albian age, comprising Unit VII represented by samples from Core 113-693A-46R and deeper, is dominated by amorphous kerogen of planktonic origin.

The kerogen of the younger unit bears from 65% to 95% vitrinite and inertinite. Brown to black, granular, amorphous material of high rank is present. Oxidation and coking are com-

Table 2. Comparative Rock-Eval data, shipboard analyses and present study, Hole 692B. S_1 = mg(HC)/g(rock), adsorbed; S_2 = mg(HC)/g(rock), pyrolytic; HI = Hydrogen Index mg(HC)/g(carbon); OI = Oxygen Index, mg(CO₂)/g(carbon).

Core, section, interval (cm)	Depth (m)	TOC (%)	S_1	S_2	HI	OI	T_{max}
692B-7R-1, 47-48	53.67	10.72	1.77	58.75	548	19.0	409
692B-7R-1, 115-116	54.35	6.30	1.04	29.18	403	20.3	416
692B-7R-2, 42-43	55.12	9.76	1.20	50.12	513	23.6	413
692B-7R-2, 112-113	55.82	16.82	1.97	58.66	349	27.5	402
692B-8R-1, 71-72	60.01	8.99	1.16	48.68	541	29.7	412
692B-8R-1, 131-132	60.61	18.41	3.21	99.34	540	28.4	406
692B-8R-2, 116-117	61.96	7.42	1.06	43.76	590	43.1	412
692B-8R-3, 126-127	63.56	9.51	1.19	55.27	581	35.5	411
692B-9R-1, 143-146	70.23	6.73	0.60	38.64	574	28.4	413
692B-10R-1, 116-117	79.66	8.20	0.73	44.78	546	31.5	415
Mean (shipboard)		10.29	1.39	52.70	518	28.7	411
Standard deviation		±4.11	±0.76	±18.80	±79	±7.1	±4
692B-7R-1, 47-48	53.67	9.97	1.31	37.71	378	40.0	418
692B-7R-1, 115-116	54.35	5.23	0.69	14.85	284	35.0	416
692B-7R-2, 42-43	55.12	8.26	1.14	30.35	367	42.0	419
692B-7R-2, 112-113	55.82	16.55	1.57	39.79	240	54.0	418
692B-8R-1, 71-72	60.01	7.84	0.99	30.04	383	54.0	421
692B-8R-1, 131-132	60.61	16.41	2.25	52.07	317	46.0	417
692B-8R-2, 116-117	61.96	6.46	0.66	25.11	389	65.0	419
692B-8R-3, 126-127	63.56	7.79	0.95	29.40	377	55.0	422
692B-9R-1, 143-146	70.23	6.82	0.89	25.20	370	27.0	423
692B-10R-1, 116-117	79.66	7.71	0.57	27.25	353	66.0	417
Mean (present study)		9.30	1.10	31.18	346	48.0	419
Standard deviation		±3.98	±0.51	±10.10	±50	±13	±2
Grand means (n = 20)		9.79	1.25	41.95	432	38.0	415
		±3.97	±0.65	±18.36	±110	±14	±5

Table 3. Further Rock-Eval data representing Unit III, Hole 629B. 1S_3 = mg(CO₂)/g(rock). 2PI = $S_1/(S_1 + S_2)$.

Core, section, interval (cm)	Depth (mbsf)	Lithology	TOC	S_1	S_2	1S_3	T_{max}	HI	OI	S_2/S_3	2PI
7R-2, 17-18	54.87	Claystone	7.85	1.06	28.75	2.17	415	366	28	13.25	0.04
8R-1, 46-47	59.76	Ash	1.29	0.07	3.23	1.54	426	250	119	2.10	0.02
8R-1, 130-131	60.60	Claystone	12.93	2.01	48.62	6.15	418	376	48	7.91	0.04
8R-2, 19-23	60.99	Claystone	8.76	1.36	40.57	3.09	416	463	35	13.13	0.03
8R-2, 25-26	61.05	Ash	1.34	0.08	3.98	1.12	422	297	84	3.55	0.02
8R-3, 40-41	62.70	Claystone	4.01	0.35	15.41	3.38	423	384	84	4.56	0.02
12R-1, 115-118	89.35	Claystone	4.04	0.27	11.60	2.36	425	287	58	4.92	0.02

mon; pyritized diatoms occur. There is no fluorescence. Vitrinite reflectance measurements, represented in Figure 4, indicate that the younger unit can be subdivided on the basis of the nature of the recycled vitrinite particle populations. Cores 113-693A-12R and -18R of early Pliocene age possess an extremely wide range of vitrinite reflectances (Fig. 4). This demonstrates sediment provenance from an extensive heterogeneous terrain possessing sedimentary strata of a diversity of thermal histories, exhibiting reflectance levels up to 3.8%, close to that of meta-anthracite, the highest defined coal rank. The same vitrinite population is recognizable in sediments at Sites 695, 696, and 697, suggesting a remarkably widespread dispersal of very diverse organic particles. It is suggested that these characteristics are compatible with subglacial erosion. It is noteworthy that the older sediments differ. The late Miocene sample from Core 113-693A-28R, at the base of the younger unit, bears kerogen which is likewise vitrinite-dominated, but which shows only a limited dispersion of values (Fig. 4). An Aptian-Albian sample (Sample 113-693A-46R-1, 21-22 cm) is similar. This suggests a source terrain of more restricted diversity.

The kerogen of the older unit, Lithological Unit VII of Aptian-Albian age, contains merely 20%-35% vitrinite and inertinite, but represents relatively high levels of organic carbon (2.99%-0.82% TOC). The dominant material is amorphous kerogen of brown, fluffy to granular appearance with orange-brown fluorescence and yellow-orange algal fragments. The amorphous kerogen is of typical planktonic type, and would be expected to yield good quality petroleum source material when mature. Rock-Eval data show, however, that oxidation has taken place, substantially degrading it, as discussed below. Minor solid bitumen and high pyrite concentrations are present.

The maturity suggested by the vitrinite population in the Aptian-Albian is surprisingly high, interpreted R_o values ranging from 0.75% to 0.83% (Table 4). This inference is supported by the thermal alteration index values of *2+. Recycled vitrinite of higher maturity is also present, rendering the recognition of primary material difficult, and posing the risk of an overestimate of actual maturity. It is feasible that a substantial proportion of the vitrinite in the Aptian-Albian section is recycled, as indicated by bimodal distributions of values in Cores 113-693A-

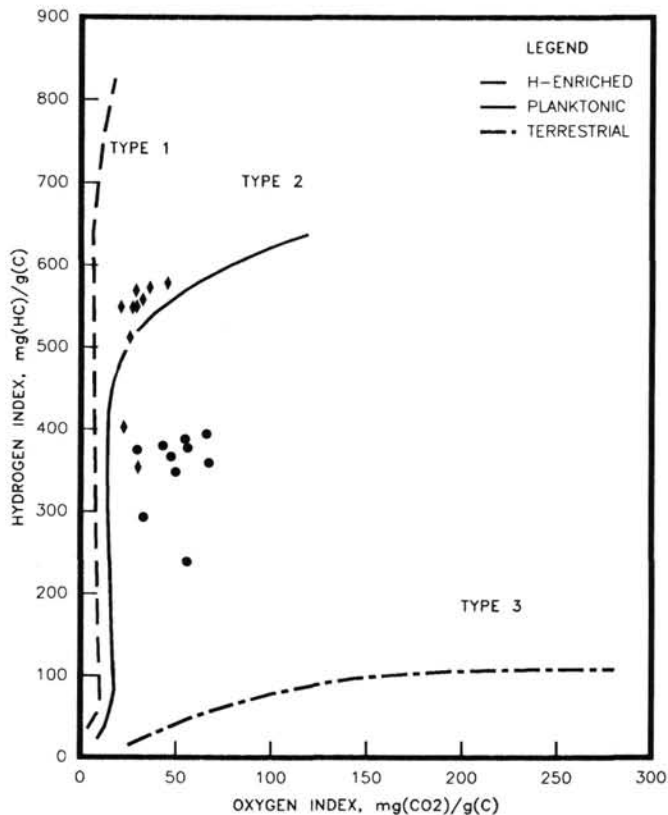


Figure 1. Rock-Eval data representing samples from Site 692. Diamond symbols = shipboard analyses; circles = authors' data. Details are presented in Table 2.

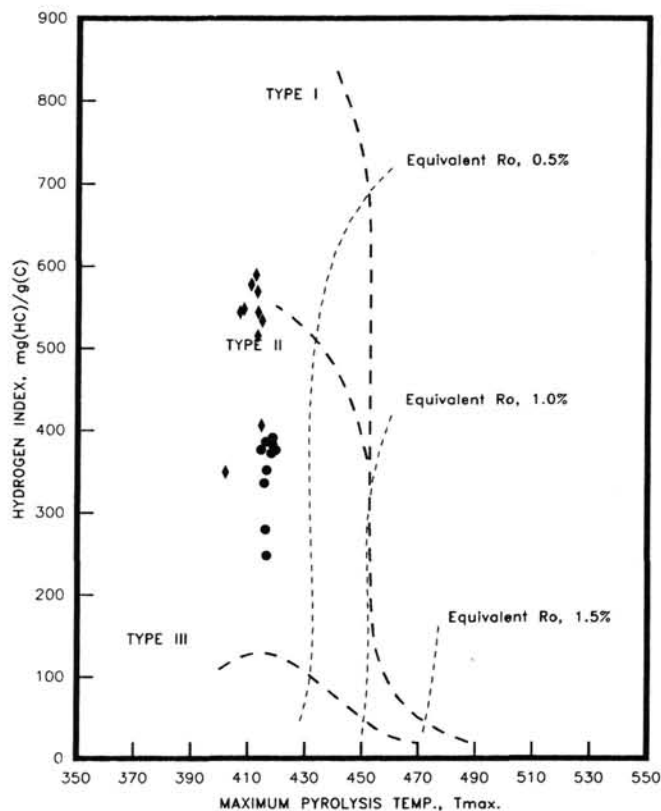


Figure 2. T_{max} and HI data from Table 2 representing shipboard analyses and those of the authors, Site 692. Symbols as in Figure 1.

Table 4. Visual kerogen data and vitrinite reflectance measurements, Holes 692B, 693A, 695A, 696B, and 697B: AMOR = amorphous kerogen; EXIN = exinite; VIT = vitrinite; INERT = inertinite; BITM = bitumen; TAI* = modified thermal alteration index based on color of kerogen; R_o = vitrinite reflectance.

Core, section interval (cm)	TOC (wt%)	Interpreted maturity		Kerogen type visual estimate (%)					Fluorescence
		R_o %	TAI*	AMOR	EXIN	VIT	INERT	BITM	
692B-7R-2, 17-18	7.85	0.43	*2	85	5	Tr	Tr	10	Medium
692B-8R-2, 19-23	8.76	0.42	*2	80	10	Tr	Tr	10	Medium
692B-9R-1, 143-146	6.82	0.49	*2	70	10	10	Tr	10	Medium
692B-12R-1, 115-118	4.04	0.62	*2	65	25	5	5	0	Low
693A-4R-3, 125-129	0.10	—	*2	15	5	65	10	5	None
693A-12R-4, 128-132	0.26	—	*2, 2+, 4-	30	5	30	35	0	None
693A-18R-3, 128-132	0.19	—	*2+, 3+, 4-	0	0	75	20	0	None
693A-28R-3, 128-132	0.10	0.72	*2+, 3	10	Tr	45	45	0	None
693A-46R-1, 21-22	—	0.77	*2+, 3-	55	10	20	10	5	ND†
693A-48R-1, 79-80	2.07	0.75	*2+	50	10	25	10	5	ND†
693A-49R-1, 44-45	2.07	0.79	*2+, 3-	60	10	10	10	10	ND†
693A-50R-2, 51-52	2.99	0.83	*2+	55	10	20	10	5	ND†
693A-51R-1, 149-150	0.82	0.77	*3	60	10	15	15	0	ND†
695A-15H-3, 120-125	0.50	0.46	*3	35	5	30	30	0	Medium
695A-36X-2, 125-129	0.47	0.41	*2+, 4-	40	Tr	30	30	0	None
695A-39X-3, 125-129	0.44	0.50	*2+, 4-	35	5	30	30	Tr	None
696B-6R-3, 125-129	0.33	—	*2, 3+	30	5	35	25	5	None
696B-23R-3, 125-129	0.16	—	*3-, 3	35	0	30	35	0	None
696B-62R-5, 125-129	0.45	—	*2	60	10	10	20	0	Low
697B-9H-3, 125-129	0.42	0.82	*2, 3+	30	Tr	35	35	0	None
697B-29X-2, 125-129	0.39	0.74	2- to 3+	40	Tr	30	30	0	None

†ND = no data.

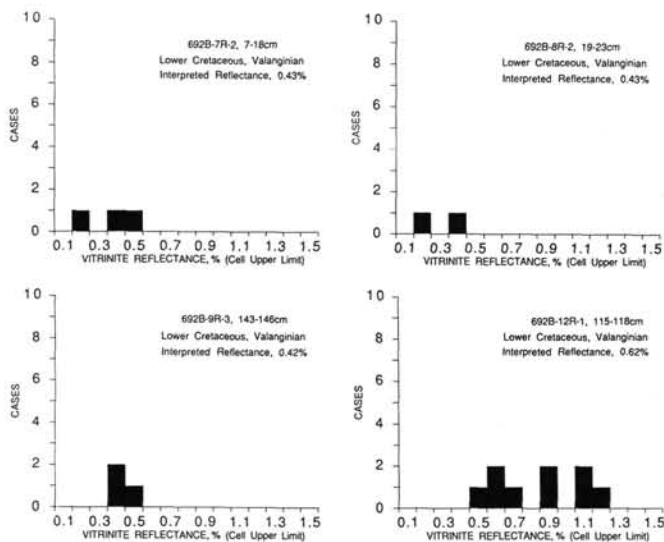


Figure 3. Vitrinite reflectance data representing selected samples from Hole 692B.

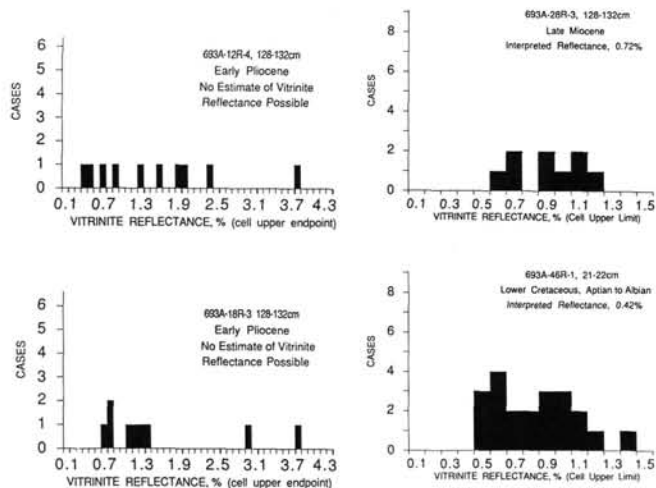


Figure 4. Vitrinite reflectance data representing selected samples from Hole 693A.

48R and -49R. The means of the lower modes in these instances are $0.60\% \pm 0.09\%$ ($n = 15$) and $0.61\% \pm 0.07\%$ ($n = 8$). Such values are in better accord with the level of $0.52\% \pm 0.10\%$ estimated for the Valanginian section of Site 692, 30 km distant.

Previously unpublished Rock-Eval data representing Site 693 are given in Table 5. The majority of Pleistocene, Pliocene, and Miocene samples (above the top of the late Oligocene in Core 113-693A-33R) contain less than 0.2% organic carbon (Table 1), and therefore were not analyzed further. Four additional samples from this interval, representing Cores 113-693B-6H, -12R, -15R, and -25R, average 0.27% TOC yet possess no detectable pyrolytic yield of hydrocarbons, giving Hydrogen Index (HI) values of zero. This is compatible with the extremely high reflectance values and the presence of spent kerogen, a refractory, volatile-free residue.

The Oligocene lithological unit, V, represented in Core 113-693A-40R behaves identically to the Miocene and younger samples, having no S_2 response.

The older stratigraphic units, VI and VII at depths greater than 397.8 mbsf, of Aptian-Albian age, also yield extremely low Rock-Eval hydrocarbon responses. Sample 113-693A-51R-1, 140-143 cm (475.70 mbsf), yielded a Hydrogen Index value of 25 mg HC/gC. Other shipboard measurements ranged from 32 to 200 with a mean of 98.3 ± 39 mg HC/gC ($n = 19$). Total organic carbon values averaged $2.12 \pm 0.88\%$.

The Rock-Eval data representing the Aptian-Albian section are principally shipboard data which contrast the results of the visual kerogen studies. Relatively high levels of organic carbon of an amorphous (planktonic) nature, observed visually, suggest good petroleum source potential. This is not confirmed by the Rock-Eval data. The mean shipboard Hydrogen Index (HI) of 98, in conjunction with the mean Oxygen Index (OI) of 42.2 mg CO_2/gC , suggest a highly mature terrestrial Type III kerogen, when considered alone. Once more employing shipboard data, the occurrence of an average T_{max} of $412^\circ C$, extremely close to the grand mean T_{max} encountered in the Valanginian at Site 692, $415^\circ C$, proves that relatively immature kerogen must be present. A suggested reconciliation of all of these observations involves anoxic sediment-water interface during the Aptian-Albian at Site 693, facilitating the bacterial destruction of lipids in the dominant sedimentary organic matter (planktonic amorphous material). Such a process is known to diminish the HI values of Type II kerogens (Deroo et al., 1983; and Herbin et al., 1984).

Sites 695, 696, and 697

Sites 695, 696, and 697 lie on the southeast margin of the South Orkney microcontinent. Water depths at the sites, 1300 m, 650 m, and 3492 m, respectively, provide a vertical transect of the water masses of the Weddell gyre, and their sediments deposited during the Paleogene and Neogene. Hole 695A reached the lower Miocene, Hole 696B the Eocene, while Hole 697A bottomed in Pliocene sediments.

Visual kerogen data are presented in Table 4, Rock-Eval measurements in Table 5, and vitrinite reflectance measurements in Figure 5.

Samples representing the Pliocene and later Miocene of Sites 696 and 697 are closely similar in their kerogen make-up. The latter comprises approximately equal parts of amorphous material, vitrinite, and inertinite. These components distinguish the Pliocene kerogens of these holes from that of Pliocene age at Site 693 which was strongly dominated by vitrinite alone. In Holes 695A, 696B, and 697A the marine amorphous fraction is brownish-black with no fluorescence, indicating that it is of a high level of maturation, was previously deeply buried, and therefore evidences sediment recycling. Traces of exinite are present having an orange fluorescence, representing reworked material of low maturity. Several populations of terrestrial organic matter (vitrinite) are present, as revealed by reflectance measurements. Vitrinite particles are oxidized in part and considered to be entirely reworked.

Core 113-696B-62R provides the only sample of Eocene age which was examined. It differs distinctly from the younger strata in its kerogen make-up, comprising dominantly amorphous planktonic material. Rock-Eval measurement showed this to be completely oxidized and bereft of petroleum-generating potential.

The vitrinite populations in sediments of Pliocene age at Sites 695 and 696 are closely similar to each other, and although mixed with organic matter of other types, are similar to that at Site 693. All of these vitrinites are characterized by extremely wide ranges of reflectance values, representing a diversity of thermal histories in the eroded sediments in the source areas (Fig. 5).

The vitrinites of Hole 697A differ from those of Holes 695A and 696B. Hole 697A is located in 3495 m of water in Jane Basin whereas the two previous sites were located on the continen-

Table 5. Rock-Eval data representing Sites 693, 694, 695, 696, and 697. See Table 2 caption for explanation.

Core, section, interval (cm)	Depth (mbsf)	TOC (wt%)	S ₁	S ₂	S ₃	T _{max} °C	S ₁ × 100/TOC [mg/g(rk)]	HI	OI	S ₂ /S ₃	PI
693A-12R-4, 128-132	104.68	0.26	0.02	0.00	0.13	354	8	0	50	0.00	1.00
693A-15R-2, 146-150	130.76	0.22	0.02	0.00	0.12	491	9	0	55	0.00	1.00
693A-25R-2, 125-129	227.35	0.36	0.03	0.00	0.14	478	8	0	38	0.00	1.00
693A-40R-2, 146-150	371.86	0.25	0.01	0.00	0.04	488	4	0	16	0.00	1.00
693A-51R-1, 140-143	475.70	0.88	0.04	0.06	0.54	321	5	7	61	0.11	0.40
693B-6H-4, 141-145	273.71	0.24	0.04	0.00	0.10	354	17	0	42	0.00	1.00
694C-22X-2, 125-129	374.75	0.71	0.06	0.04	0.53	330	8	6	75	0.08	0.60
695A-3H-4, 125-129	18.15	0.46	0.07	0.02	0.22	304	15	4	48	0.09	0.78
695A-9H-2, 125-129	72.75	0.46	0.09	0.11	0.23	307	20	24	50	0.48	0.45
695A-15H-3, 120-125	122.40	0.50	0.07	0.00	0.21	272	14	0	42	0.00	1.00
695A-19X-4, 125-129	153.05	0.59	0.16	0.62	0.36	409	27	105	61	1.72	0.21
695A-22X-3, 125-129	180.75	0.33	0.06	0.06	0.09	331	18	18	27	0.67	0.50
695A-25X-3, 125-129	200.15	0.63	0.07	0.05	0.46	347	11	8	73	0.11	0.58
695A-36X-2, 125-129	295.55	0.47	0.02	0.00	0.04	219	4	0	9	0.00	1.00
695A-39X-3, 125-129	316.25	0.44	0.05	0.09	0.38	328	11	20	86	0.24	0.36
696A-5H-3, 125-129	35.45	0.46	0.11	0.11	0.15	298	24	24	33	0.73	0.50
696B-3R-3, 125-129	90.45	0.42	0.03	0.00	0.33	272	7	0	79	0.00	1.00
696B-6R-3, 125-129	119.45	0.33	0.05	0.03	0.21	302	15	9	64	0.14	0.63
696B-20R-2, 125-129	233.85	0.42	0.05	0.13	0.17	382	12	31	40	0.76	0.28
696B-23R-3, 125-129	264.35	0.16									
696B-26R-2, 125-129	291.75	0.54	0.07	0.02	0.12	312	13	4	22	0.17	0.78
696B-34R-1, 125-129	367.55	0.65	0.12	0.45	0.10	395	18	69	15	4.50	0.21
696B-62R-5, 125-129	642.06	0.45	0.04	0.05	0.41	426	9	11	91	0.12	0.44
697A-3H-4, 125-129	17.05	0.42	0.05	0.00	0.46	323	12	0	110	0.00	1.00
697B-3H-4, 125-129	42.85	0.48	0.09	0.04	0.48	272	19	8	100	0.08	0.69
697B-6H-2, 125-129	68.95	0.47	0.12	0.07	0.43	326	26	15	91	0.16	0.63
697B-9H-3, 125-129	99.65	0.42	0.06	0.05	0.37	303	14	12	88	0.14	0.55
697B-13X-3, 125-129	132.85	0.43	0.07	0.10	0.28	353	16	23	65	0.36	0.41
697B-16X-4, 125-129	163.25	0.36	0.04	0.03	0.33	291	11	8	82	0.09	0.57
697B-19X-3, 125-129	190.85	0.42	0.06	0.08	0.33	387	14	19	79	0.24	0.43
697B-22X-2, 125-129	218.25	0.31	0.03	0.04	0.12	296	10	13	39	0.33	0.43
697B-26X-2, 125-129	256.95	0.35	0.30	0.00	0.25	218	86	0	71	0.00	1.00

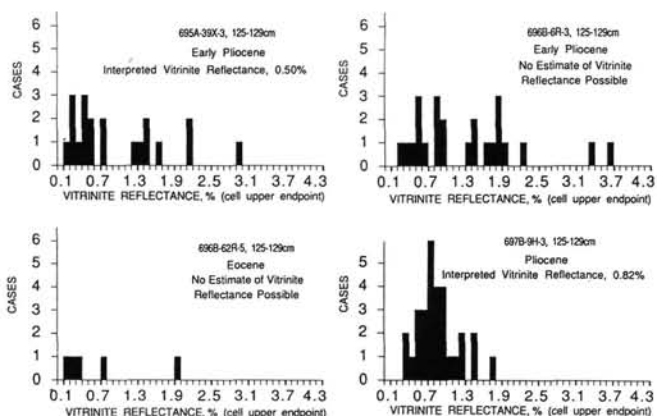


Figure 5. Vitrinite reflectance data representing samples from Holes 695A, 696B, and 697B.

tal slope at depths of 1300 m and 650 m, respectively. The difference is apparent in Figure 5 showing the substantial range of reflectances in Sections 113-695A-39X-3 and 113-696B-6R-3, up to R₀ 3.75%, but a relatively limited range, up to R₀ 1.83%, in a representative Pliocene sample, 113-697B-9H-3, 125-129 cm.

In view of the glaciated nature of the sediment source terrain during the Miocene-Pliocene it is highly improbable that any vitrinite particles are truly primary. The lower reflectance material could represent reworked Eocene vitrinite, during which time a substantial flora existed in east Antarctica (Mohr, this volume, chapter 36). Furthermore, no means is available to definitively recognize primary vitrinite in the presence of unoxidized or unaltered recycled vitrinite. For this reason vitrinite studies are un-

able to contribute to the chronology and understanding of climatic deterioration in Antarctica.

Rock-Eval data representing samples from the three sites are shown in Table 5. Values of Hydrogen Indices are all below 98 mg HC/gC, commonly below 20. No petroleum potential is therefore indicated. Highly variable T_{max} values are compatible with the varied and mixed natures of the kerogens as indicated by microscopy.

COMPARISONS OF ORGANIC-RICH CRETACEOUS STRATA IN THE ATLANTIC OCEAN BASIN

Three characteristics of kerogen-rich Valanginian strata in the Weddell Sea provide interesting comparisons with those of other sites in the Atlantic Ocean. Figure 6 (Dean and Arthur, 1986) shows locations of occurrence of Cretaceous "black shales" as encountered at previous DSDP sites. The comparisons to be made can be described under three headings: lithology, carbon and sulfur isotope ratios, and petroleum potential.

Lithology

The Cretaceous "black shales" of the Weddell Sea are unique in that they do not exhibit alternations of light and dark bands, that is, cyclic sedimentation. Two formations bearing black, laminated, organic carbon-rich strata are recognized in the eastern and western North Atlantic: the Lower Cretaceous Blake-Bahama Formation, and the Upper Cretaceous Hatteras Formation (Jansa et al., 1979). Both exhibit cyclic sedimentation and color banding. The Blake-Bahama Formation occurs at Sites 99, 100, 105, 387, and 391 in the North American Basin, at Sites 535 and 540 in the eastern Gulf of Mexico, and at Site 367 in the Cape Verde Basin in the eastern Atlantic. At Site 367 it is represented by interbedded, laminated, dark-olive to

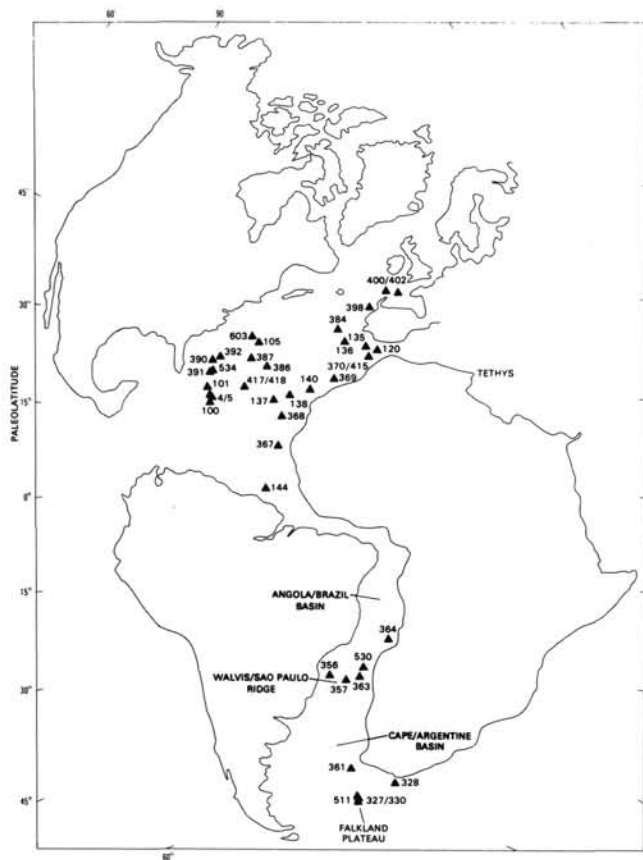


Figure 6. DSDP sites at which Cretaceous sediments rich in organic carbon were encountered. From Dean and Arthur, 1986.

black marlstone, and bioturbated white- to light-gray limestone. The Hatteras Formation at Site 367 is represented by interbedded gray-green claystone and black shale of Aptian to Turonian age. Equivalent units are recognized in the western North Atlantic at DSDP Sites 4, 5, 101, 105, 386, 391, and 398, and in the eastern North Atlantic at Sites 135, 137, 138, 167, 368, 398, 400, and 402 (Arthur, 1979; Tissot et al., 1979, 1980).

Both the Blake-Bahama and Hatteras Formations represent cyclic sedimentation and/or alternations of higher and lower levels of dissolved oxygen at the sediment-water interface. The Neocomian cycles generally comprise pelagic carbonates and marls. Thierstein (1979) suggested that a sudden rise in the carbonate compensation depth of the order of 2 km at the end of the Lower Cretaceous resulted in the subsequent accumulation of dominantly argillaceous sediments over most of the Atlantic Ocean floor, represented by the shales of the Hatteras Formation. These are also cyclic in nature. In both formations the periodicities of the cycles are estimated at between 10,000 and 50,000 yr (Dean and Gardner, 1982), with an average close to 50,000 yr in the Hatteras Formation of Site 367 (Dean et al., 1978).

Lithological cycles are closely coupled to variations in organic carbon content. In the Lower Cretaceous of Site 367 the geometric mean of nine determinations of total organic carbon in light carbonate laminae is 3.2%, while in the black marls (nine analyses) it is 5.5% (Dean and Gardner, 1982). Similarly, in the Hatteras Formation, total organic carbon averages 0.31% in the green shales and 5.3% in the black bands. In both formations, wherever found, similar cyclicity in lithological properties and organic carbon contents are observed. Cycles are of the order of 2-50 cm in thickness.

The interbedding of sediments alternately rich and poor in organic carbon requires a mechanism which causes periodic anoxic or dysoxic conditions at the seafloor. Three processes have been invoked to explain Cretaceous cyclic anoxia: periodic oceanic stagnation (anoxic events), expansion of oxygen-minimum zones, and variations in oxygen demand at the depositional site dependent upon the rate of sedimentation of organic detritus. The first two hypotheses were developed by Schlanger and Jenkyns (1976), Ryan and Cita (1977), also Fischer and Arthur (1977). The third mechanism was proposed by Dean and Gardner (1982). All of these concepts owe much to the work of Hallam (1967). Dean and Gardner (1982) also concur with the conclusion of Jansa et al. (1979) that turbidity current emplacement caused the periodic delivery of organic matter rich sediment into oxygenated abyssal environments in certain instances, accounting for cyclic alterations of total organic carbon.

The remarkable aspect of both the Valanginian at Site 692 and the Aptian-Albian at Site 693 is the absence of macroscopic cyclicity, either in lithology or total organic carbon. The occurrence of continuous anoxia at Site 692 during the accumulation of the recovered 22.18 m of sediment (which contains only Type II kerogen and bears no oxidized laminae) evidently required a depositional setting which differed from those elsewhere throughout the Atlantic Ocean during the Cretaceous. A mechanism which continuously precluded both oxygenation of the bottom waters and the arrival of turbidity currents from shallower regions of the continental margin is required. Such would be provided by a series of silled basins in progressively deeper waters, the proximal basins acting as sediment traps for the distal ones. One of the latter, with its sill located permanently within the oxygen minimum zone of Valanginian time, could have provided an appropriate depositional setting. Basins of the configurations described, of Tertiary to Recent age, occur in the continental borderland off the coast of California (Emery, 1960), and have accumulated substantial thicknesses of euxinic pelagic sediments bearing entirely Type II kerogen.

Carbon and Sulfur Isotope Ratios of Kerogens

Paired isotope ratio values (carbon and sulfur) provide significantly more useful data for potential use in petroleum and source kerogen correlation than do either alone (Thompson et al., in press). Four sets of analyses representing Type II kerogens of Valanginian age at Site 692 are given in Table 6. The analyzed material was separated by acidification and flotation. It is probable that incomplete removal of pyrite (which is generally extremely isotopically light in sulfur) led to the very negative $\delta^{34}\text{S}$ value in Core 113-692B-12R.

It is of interest to compare these data with values representing other Cretaceous oceanic sediments containing Type II kerogen, such as those of Sites 535 and 540, DSDP Leg 77 (first author's unpublished data), shown in Table 7. At Site 535, located northwest of Cuba in the eastern Gulf of Mexico, a reasonably close agreement with Site 692 in $\delta^{13}\text{C}$ (kerogen) is found for the

Table 6. Carbon and sulfur isotope ratios of kerogens, Site 692. Carbon isotope ratios, $\delta^{13}\text{C}/\text{ml}$, versus PDB. Sulfur isotope ratios, $\delta^{34}\text{S}$, per mil versus CDT.

Core, section, interval (cm)	Depth (mbsf)	Isotope ratios	
		$\delta^{13}\text{C}$	$\delta^{34}\text{S}$
692B-7R-2, 17-18	54.87	-30.0	-2.2
692B-8R-2, 19-23	60.99	-30.4	-6.0
692B-9R-1, 143-146	70.23	-30.6	-7.3
692B-12R-1, 115-118	89.35	-29.5	-27.0

Table 7. Carbon and sulfur isotope ratios of kerogens, Holes 535 and 540, DSDP Leg 77. Authors' unpublished data.

Core, section, interval (cm)	Hydrogen index	$\delta^{13}\text{C}$ (kerogen)	$\delta^{34}\text{S}$ (kerogen)	Age
535-35-5, 45-48	229	-26.8	-9.5	Albian
535-41-5, 126-129	421	-26.0	-7.6	Albian
535-44-1, 118-122	268	-27.0	-13.9	Aptian
535-47-1, 97-100	309	-27.9	-17.3	Hauterivian
535-53-2, 0-5	352	-27.7	-2.0	Hauterivian
535-60-2, 16-20	385	-26.9	-4.3	Hauterivian
535-70-5, 137-140	281	-28.7	-6.0	Valanginian
535-77-1, 127-130	173	-28.6	-8.2	Berriasian
540-29-2, 0-3	74	-25.1	-3.7	Cenomanian
540-42-2, 30-35	400	-25.2	-11.6	Vraconian
540-42-2, 40-42	525	-27.0	-11.4	Vraconian
540-59-1, 14-18	128	-24.6	-19.7	Late Albian
540-59-1, 29-31	4	-26.5	-11.6	Late Albian
540-73-3, 56-60	19	-26.8	-9.8	Mid Albian

Valanginian and Berriasian. Both older and younger Cretaceous intervals exhibit substantially isotopically heavier kerogen.

Petroleum Potential

The petroleum potential of sedimentary rocks has been defined in terms of the results of a standardized pyrolysis process (Rock-Eval analysis) by Espitalié et al. (1977a, 1977b). Potential is represented by the sum of the thermally vaporizable and pyrolytic hydrocarbon yields ($S_1 + S_2$) expressed on the basis of rock weight units, mg of hydrocarbons per g of rock, or for purposes of regional appraisal, in kg/tonne. Espitalié's scale of merit is represented by the following:

Potential	kg/tonne
Very weak	0.01-0.50
Weak	0.51-2.00
Intermediate	2.01-5.00
Good	5.01-20.0
Very good	>20.0

As a practical matter, a level above 2.0 kg/tonne is considered to be significant.

Major petroleum source sequences yield values such as the following in units of kg/tonne: the Kimmeridgian of the North Sea and the Jurassic of Saudi Arabia, 50; the Lower Lias of the Paris basin, 20; the Oxfordian of the Aquitaine basin, 30; and the Cretaceous carbonates of North Africa, 10. Extreme values are represented by the Permian Irati shale, 100 kg/tonne, and the Green River Shale (Eocene), 200 kg/tonne (Deroo and Herbin, 1980).

For comparison, the Valanginian of Site 692 (Table 2) possesses an average potential of 43.2 kg/tonne over a penetrated thickness of 44.7 m. There was no indication that the recovered cores represented an approach to the base of the section. On the contrary, DSDP Legs 36 and 71 showed that sediments similar to Unit III at Site 692, those exhibiting anoxia, were developed on the Falkland Plateau over the entire Kimmeridgian-Albian interval. The facies could therefore be much thicker than 44.7 m, conceivably extending to the continental margin unconformity, 600 ms two-way travel time, approximately 1.1 km, below the penetrated section at Site 692.

A comparison may also be made between Unit III, Site 692, and other Atlantic Ocean sections. In the southern Atlantic, Cretaceous black shale facies possess modal percentages of total organic carbon and modal petroleum potentials as follows: at Site 361 (Leg 40) in the Cape basin, 3% TOC and 8 kg/tonne;

at Site 364 (Leg 40) in the Angola basin, 10% TOC and 80 kg/tonne. At Site 511, Leg 71, comparable values were 4% and 20 kg/tonne, representing the Falkland Plateau. The latter area was close to Site 692 at the time of sedimentation, but the sites were separated by an active plate margin (Lawver et al., 1985).

A detailed comparison may be made with northern Atlantic sites for which the data of Table 8 were compiled by Deroo and Herbin (1980).

The mean petroleum potential of the Neoconian strata of Site 692 is exceeded only by that of the Albian and Turonian sections of Site 367 off Cape Verde in the Northern Atlantic, and by the Cretaceous of Site 364 in the Angola basin in the southern Atlantic. The potential at Site 692, 43.2 kg/tonne approaches that of several of the notable petroleum source rocks of the world: the Kimmeridgian of the North Sea and the Jurassic of Saudi Arabia.

CONCLUSIONS

A sequence of "black shales" of Valanginian age was penetrated over an interval of 44.7 m in Hole 692B, off Kapp Norvegia in the Weddell Sea. The sequence is unique compared to other known sections of Cretaceous "black shales," particularly the Lower Cretaceous Blake-Bahama Formation which is most closely analogous, in failing to exhibit macroscopic cycles of sedimentation. Conditions of sedimentation were therefore anoxic and extremely uniform, suggestive of deposition in a silled basin. The petroleum source potential is extraordinarily high. Total organic carbon averaged $9.79\% \pm 3.97\%$ in a representative suite of ten samples analyzed in duplicate. The Hydrogen Index, measured by Rock-Eval, was 432 ± 110 mg (hydrocarbons)/g (carbon), and the total pyrolytic yield (S_2) was 41.95 ± 18.36 mg(hydrocarbons)/g(rock), or kg/tonne.

The Aptian-Albian strata of Hole 693A contain solely amorphous kerogen of planktonic origin, analogous to that of the Valanginian, but in this instance bereft of petroleum potential due to syndepositional oxidation. One sample of Eocene kerogen, from Hole 696B, was examined. Minor amounts of vitrinite occur in a kerogen matrix identical to that described for the Aptian-Albian in Hole 693A.

The younger Paleogene and Neogene strata, sampled in Holes 693A, 695A, 696B, and 697B possess kerogens dominated by vitrinite and inertinite of an extremely wide range of maturities (up to R_0 3.84%), encountered on both sides of the Weddell Sea. The wide range is attributed to kerogen recycling from a thermally heterogeneous terrain.

This study did not address the potential relationship between kerogen type, climatic deterioration, and glaciation. The dearth of primary terrestrial detritus (low maturity vitrinite) in the younger Tertiary section is noteworthy, however.

ACKNOWLEDGMENTS

This work was supported by the JOI U.S. Science Advisory Committee (USSAC). The latter is associated with the Ocean Drilling Program and is sponsored by the National Science Foundation as well as by the Joint Oceanographic Institutions, Inc. The findings and conclusions expressed are those of the authors and do not necessarily reflect the views of the National Science Foundation, the Joint Oceanographic Institutions, Inc., or Texas A&M University.

REFERENCES

- Arthur, M. A., 1979. North Atlantic Cretaceous black shales: The record at Site 398 and a brief comparison with other occurrences. *In* Sibuet, J. C. and Ryan, W.B.F., et al., *Init. Repts. DSDP*, 47, Pt. 2: Washington (U.S. Govt. Printing Office), 719-751.
- Barker, P. F., Kennett, J. P., et al., 1988. *Proc. ODP, Init. Repts.*, 113: College Station, TX (Ocean Drilling Program).

Dean, W. A. and Gardner, J. V., 1982. Origin and geochemistry of redox cycles of Jurassic to Eocene age, Cape Verde basin (D.S.D.P. Site 367), continental margin of northwest Africa. In Schlanger, S. O., and Cita, M. B. (Eds.), *Nature and Origin of Cretaceous Carbon-rich Facies*: New York (Academic Press), 55-78.

Dean, W. E., and Arthur, M. A., 1986. Origin and diagenesis of Cretaceous organic-carbon-rich lithofacies in the Atlantic Ocean. In Mumpton, F. A., (Ed.), *Studies in Diagenesis*, U.S. Geol. Surv. Bull., 1578:97-128.

Dean, W. E., Gardner, J. V., Jansa, L. F., Cepek, P., and Leibold, E., 1978. Cyclic sedimentation along the continental margin of northwest Africa. In Lancelot, Y., Seibold, E., et al., *Init. Repts. DSDP*, 41: Washington (U.S. Govt. Printing Office), 965-989.

Deroo, G., and Herbin, J. P., 1980. Bilan des culminations de matière organique pétrolière dans le Crétacé de forage DSDP en Atlantique nord. In Burollet, P. F., and Ziegler, V. (Eds.), *Colloque C2, Ressources Énergétiques, 26th Internat. Geol. Cong.* Paris (Editions Technip), 327-333.

Deroo, G., Herbin, J. P., and Roucaché, J., 1983. Organic geochemistry of Upper Jurassic-Cretaceous sediments from Site 511, Leg 71, western south Atlantic. In Ludwig, W. J., Krashennikov, V. A., et al., *Init. Repts. DSDP*, 71: Washington (U.S. Govt. Printing Office), 1001-1013.

Emery, K. O., 1960. *The Sea off Southern California*. New York (John Wiley and Sons).

Espitalié, J., Laporte, J. L., Madec, M., Marquis, F., Leplat, P., Paulet, J., and Boutefou, A., 1977a. Méthode rapide de caractérisation des roches mères, de leur potentiel pétrolier, et de leur degré d'évolution. *Rev. Inst. Fr. Pétrol.*, 32:23-42.

Espitalié, J., Madec, M., Tissot, B., Manning, J. J., and Leplat, P., 1977b. Source rock characterization method for petroleum exploration. *Proc. Offshore Technol. Conf.*, 3:439-443.

Fischer, A. G., and Arthur, M. A., 1977. Secular variations in the pelagic realm. In Cook, H. E., and Enos, P. (Eds.), *Deep Water Carbonate Environments*. Soc. Econ. Paleontol. Mineral. Spec. Publ., 25:19-50.

Hallam, A., 1967. The depth significance of shales with bituminous laminae. *Mar. Geol.*, 5:481-494.

Herbin, J. P., Deroo, G., and Roucaché, J., 1984. Organic geochemistry of Lower Cretaceous sediments from Site 535, Leg 77, Florida Straits. In Buffler, R. T., Schlager, W., et al., *Init. Repts. DSDP*, 77: Washington (U.S. Govt. Printing Office), 459-475.

Jansa, L. F., Enos, P., Tucholke, B. E., Gradstein, F. M., and Sheridan, R. E., 1979. Mesozoic-Cenozoic sedimentary formations of the North Atlantic basin, western North Atlantic. In Talwani, M., Hay, W. W., and Ryan, W.B.F. (Eds.), *Deep Drilling Results in the Atlantic Ocean: Continental Margins and Paleoenvironment*, Am. Geophys. Un., Mar. Environ. Ser., 3:1-57.

Lawver, L. A., Sclater, J. G., and Meinke, L., 1985. Mesozoic and Cenozoic reconstructions of the South Atlantic. *Tectonophysics*, 114: 233-254.

Ryan, W.B.F., and Cita, M. B., 1977. Ignorance concerning episodes of oceanwide stagnation. *Mar. Geol.*, 23:197-215.

Schlanger, S. O., and Jenkyns, H. C., 1976. Cretaceous oceanic anoxic events: causes and consequences. *Geol. Mijnbouw*, 55:179-184.

Thierstein, H. R., 1979. Paleooceanographic implications of organic carbon and carbonate distribution in Mesozoic deepsea sediments. In Talwani, M., Hay, W. W., and Ryan, W.B.F. (Eds.), *Deep Drilling Results in the Atlantic Ocean: Continental Margins and Paleoenvironment*. Am. Geophys. Un., Mar. Environ. Ser., 3:249-274.

Thompson, K.F.M., Kennicutt, M. C., II, and Brooks, J. M., in press. Classification of offshore Gulf of Mexico oils and gas-condensates. *AAPG Bull.*

Tissot, B., Deroo, G., and Herbin, J. P., 1979. Organic matter in Cretaceous sediments of the North Atlantic: Contributions to sedimentology and paleogeography. In Talwani, M., Hay, W. W., and Ryan, W.B.F. (Eds.), *Deep Drilling Results in the Atlantic Ocean: Continental Margins and Paleoenvironment*. Am. Geophys. Un., Mar. Environ. Ser., 3:362-374.

Tissot, B., Demaison, G., Masson, P., Delteil, J. R., and Combaz, A., 1980. Paleoenvironment and petroleum potential of middle Cretaceous black shales in Atlantic basins. *AAPG Bull.*, 64:2051-2063.

Date of initial receipt: 1 March 1989
 Date of acceptance: 27 September 1989
 Ms 113B-164

Table 8. Mean petroleum potential and thickness data for northern Atlantic Cretaceous black shale sections. (After Tissot et al., 1980; and Deroo and Herbin, 1980.)

Site	Petroleum potential (kg/tonne)	Thickness (m)	Petroleum potential (kg/tonne)	Thickness (m)	Petroleum potential (kg/tonne)	Thickness (m)
	Post-Cenomanian		Albian-Cenomanian		Pre-Albian	
105	—	—	5.10	110	1.65	210
137	0.65	65	0.55	116	—	—
367	93.20	205	33.00	120	5.30	220
369	—	—	23.10	35	22.50	30
370	—	—	1.40	120	2.10	380
386	0.15	30	5.10	298	—	—
387	0.45	45	8.70	115	6.25	190
391	—	—	0.50	252	1.50	346
398	22.50	1	0.30	464	0.20	228
400	0.01	30	0.80	45	0.05	53
402	—	—	0.20	205	1.40	90
417	0	55	8.00	70	4.50	4
418	—	—	8.00	64	—	—